ACS APPLIED POLYMER MATERIALS

pubs.acs.org/acsapm
Article

Micellar Transfer Hydrogenation Catalysis in Water with Monocarbonyl Ruthenium(II)-poly(vinylphosphonate)-Containing Polymers: Achieving Reduction of Biomass-Derived Aldehydes

Denise Lovison,[§] Philipp Weingarten,[§] Alexandra Sebeschuk, Bernhard Rieger,* and Angela Casini*

Cite This: *ACS Appl. Polym. Mater.* 2024, 6, 13855−13864
Read Online

ACCESS | Metrics & More | Article Recommendations | Supporting Information

ABSTRACT: With the aim to build a supramolecular organometallic catalyst for transfer hydrogenation (TH) reactions of hydrophobic substrates, micellar architectures of different sizes were obtained using amphiphilic diblock copolymers (BCPs) tethered to a Ru(II) monocarbonyl complex. An end-group functionalization strategy was employed to incorporate a bipyridyl end-group, used to further coordinate the cationic ruthenium fragment, to amphiphilic poly(2-vinylpyridine)-*b*-poly(diethyl vinylphosphonate). Owing to their amphiphilic character, the polymers form spherical micelles in water, which were characterized by different spectroscopic and analytical methods at different pH values and temperatures. The most suitable core−shell micellar system could level the catalytic activity of the ruthenium complex toward hydrophobic and biomass-derived aldehydes, which could be successfully reduced to the corresponding alcohols in water using potassium formate as a hydride source. Depending on the substrate's hydrophobicity and concentration, the catalytic activity varied significantly. In addition, the polymer's properties hardly changed during catalysis, facilitating effective recycling until the third catalytic cycle.

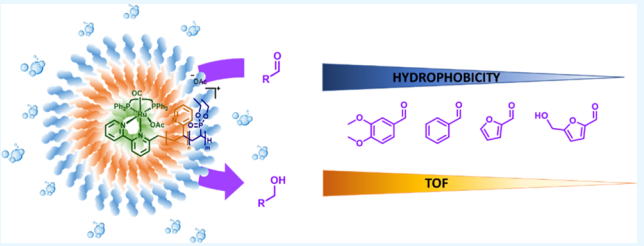

KEYWORDS: *ruthenium, diblock copolymers, micelles, transfer hydrogenation, aldehydes, catalysis*

INTRODUCTION

Nowadays, homogeneous catalysis has reached extremely high levels of selectivity. Nevertheless, several efficient catalytic systems need to be revisited due to the increasingly stringent requirements of green chemistry principles. In particular, the possibility of performing reactions in water is still of great importance due to the benign, abundant, economical, and environmentally friendly nature of this solvent. Despite these advantages, water use in catalysis has found limited application since many water-insoluble (apolar) substrates are difficult targets for aqueous-phase reactions. Nevertheless, since the seminal work of Breslow in 1980, a large variety of organic reactions have been proven to take place in aqueous media, sometimes with outstanding enhancements, such as faster reaction rates and greater selectivity compared with results obtained using classic organic solvent-based systems.[1] Recently, we reported on a family of Ru(II) monocarbonyl compounds of general formula $[RuCO(dppb)(N^{\wedge}N)(OAc)]^{n}$ (n = +1, 0; dppb = 1,4-bis(diphenylphosphino)butane, OAc = acetate; N^N = bidentate N-donor ligands) (Figure 1), which can catalyze the regioselective reduction of nicotinamide adenine dinucleotide (NAD^{+}) to 1,4-dihydronicotinamide adenine dinucleotide (1,4-NADH) in aqueous solution with sodium formate as a hydride source, as well as the reverse oxidation of 1,4-NADH.[2] This reactivity is likely to account for the observed anticancer effects of this family of compounds *in vitro*.[3−6] Interestingly, the titled transfer hydrogenation (TH) catalysis can only occur in water and not in other organic solvents, pointing toward a key role of water molecules during the TH pathway. To broaden the scope of the Ru(II) monocarbonyl catalysts to include different organic substrates, we decided to apply a supramolecular approach.

In this context, micelles represent an interesting host choice as many commercially available amphiphiles can provide the desired reaction vessels by self-assembly.[7,8] The micellar approach can overcome the phase transfer limitations for water-organic catalytic systems and has been employed in many classical catalytic transformations,[9] in particular for a wide range of reactions promoted by metal complexes or organometallic species, as well as in photochemistry and photocatalysis.[10] To achieve stable dispersion in aqueous environments, core−shell micelle architectures are typically obtained using amphiphilic diblock copolymers (BCPs). In this case, the outer shell consists of hydrophilic blocks while the

Received: September 3, 2024
Revised: October 28, 2024
Accepted: October 29, 2024
Published: November 7, 2024

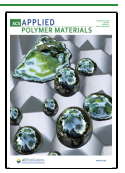

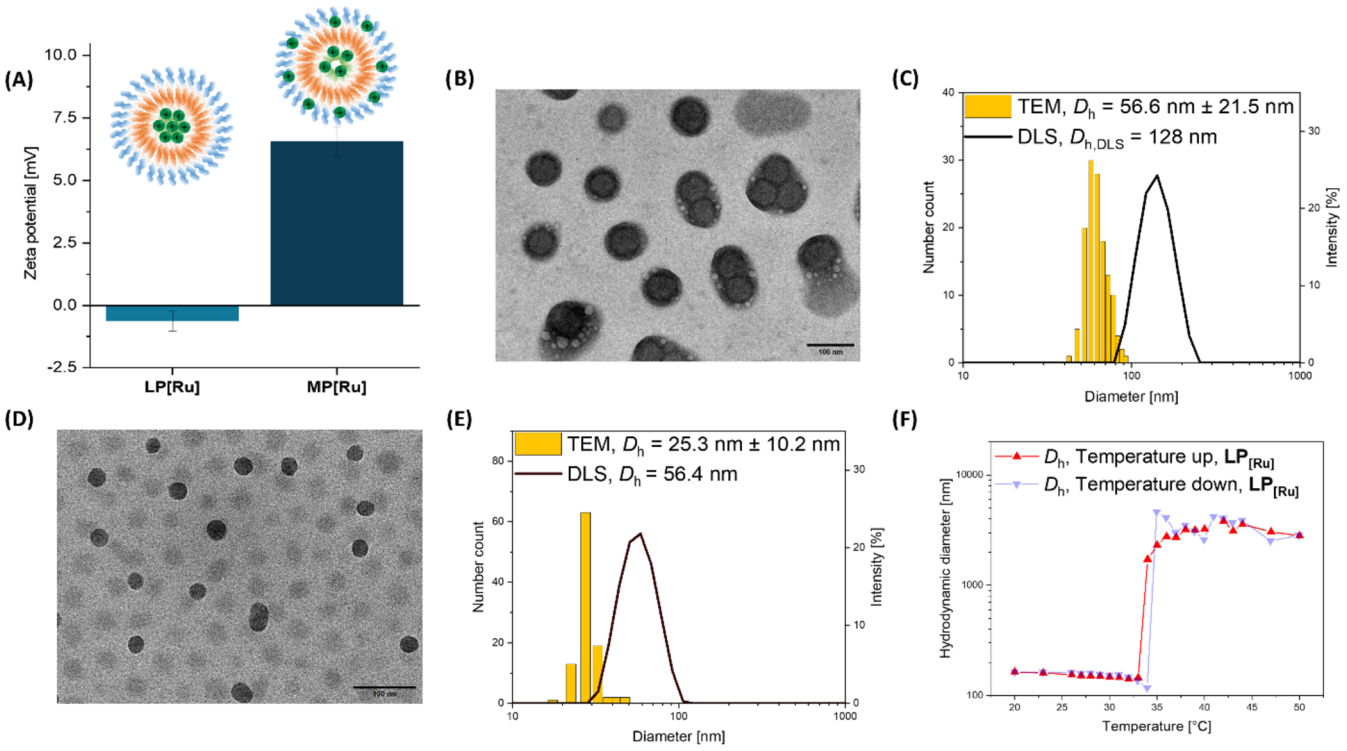

Figure 1. Physicochemical properties of [Ru]-functionalized micelles. (A) ζ-Potential determination of $\mathbf{LP}_{[Ru]}$ and $\mathbf{MP}_{[Ru]}$ in ddH_2O. (B) TEM image of $\mathbf{LP}_{[Ru]}$ micelles at pH 7.4 (scale bar = 100 nm). (C) TEM size distribution (yellow) and the result of DLS (black) of $\mathbf{LP}_{[Ru]}$. (D) TEM image of $\mathbf{MP}_{[Ru]}$ micelles at pH 7.4 (scale bar = 100 nm). (E) TEM size distribution (yellow) and the result of DLS (black) of $\mathbf{MP}_{[Ru]}$. (F) Size distribution of $\mathbf{LP}_{[Ru]}$ at various temperatures (red: temperature up; blue: temperature down). All experiments (except ζ-potential) were performed at 1 mg mL^{-1} in 100 mM PBS buffer at pH 7.4.

inner core is stabilized by hydrophobic interactions.[11,12] Transition-metal-based catalysts are frequently immobilized on polymers using either a ligand exchange reaction or via the attachment of the catalytically active complex using a thiol−ene reaction or Steglich conditions.[13−21] A number of studies have also described the use of micelles to facilitate TH catalysis by metal complexes in water.[22−24] For example, substrate-selective TH of ketones using rhodium complexes immobilized on a photoresponsive nanoreactor has been recently reported.[25] Moreover, the catalytic activity of micellar Ru-based catalysts in water-phase transfer hydrogenation of (hydrophobic) ketones and its enhancement by ionic cosurfactants has also been described.[26,27] Since surfactants offer a limited tailoring potential without altering their intrinsic structure, polymer-based micelles, in general, profit from higher stability and structural versatility, while the potential cargo capacity for substrates can be enhanced by tailoring the polymer microstructure. For example, poly(2-alkyl oxazoline)-based block copolymers could be functionalized with a Co-porphyrin and a Rh-based catalyst to generate chiral alcohols from phenyl acetophenone in tandem hydration and hydrogenation reactions.[16] Additionally, amphiphilic phosphine-containing core−shell polymers could facilitate Rh-catalyzed hydrogenation of alkenes.[28] Both examples emphasize the importance of both the end-group and side-chain functional ability of the polymers in establishing successful catalysis.

Here, the synthesis of a ruthenium-functionalized AB-type BCP, which can form micellar vessels in an aqueous environment in a facile manner, is reported. The Ru(II) catalytic fragment [RuCO(dppb)(N^N)(OAc)] has been tethered to the polymer via the bipyridyl (N^N) end-group, providing a facile strategy to introduce the catalyst for TH into the polymer.[2,29] The BCP framework is composed of 2-vinylpyridine (2VP) and diethyl vinylphosphonate (DEVP) copolymerized by rare-earth metal-mediated group-transfer polymerization (REM-GTP).[30−33] A crucial advantage of the applied REM-GTP is the introduction of functional end-groups, such as alkynes, alcohols, or bipyridyl moieties, through polymerization.[34−36] The polymers feature narrow polydispersities and high initiation efficiencies, and the hydrophobic and pH-responsive poly(2-vinylpyridine) (P2VP) block provides buffering capacity between pH values 4 and 6.[37] Copolymerized poly(diethyl vinylphosphonate) (PDEVP) ultimately gives temperature-responsive and amphiphilic properties to BCP.

Three P2VP-*b*-PDEVP BCPs featuring the bipyridyl end-group and different overall sizes were synthesized. The Ru(II)-functionalized P2VP-*b*-PDEVP BCPs were characterized by different methods, including size exclusion chromatography (SEC), nuclear magnetic resonance spectroscopy (NMR), Nile red assay for the determination of the critical micelle concentration (CMC), inductively coupled plasma mass spectrometry (ICP-MS), dynamic light scattering (DLS) and ζ-potential, and transmission electron microscopy (TEM) under various pH values. The developed ruthenium-micellar systems were demonstrated to be moderately active as catalysts toward the reduction of hydrophobic biomass-derived aldehydes in aqueous media, namely, benzaldehyde, furfural, 5-hydroxymethylfurfural, and 3,4-dimethoxybenzaldehyde, using formate as hydride source. Notably, the TH activity of the systems showed great dependence on the pH value of the media and the hydrophobicity of the substrates. Finally, the

https://doi.org/10.1021/acsapm.4c02762
ACS Appl. Polym. Mater. 2024, 6, 13855−13864

Scheme 1. Fabrication of Catalytic Ru(II)-Containing Micelles. Preparation of Ruthenium-Functionalized BCPs Using REM-GTP and Subsequent Reaction with the Ru(II) Precursor [Ru(η^1-OAc)(η^2-OAc)CO(dppb)]

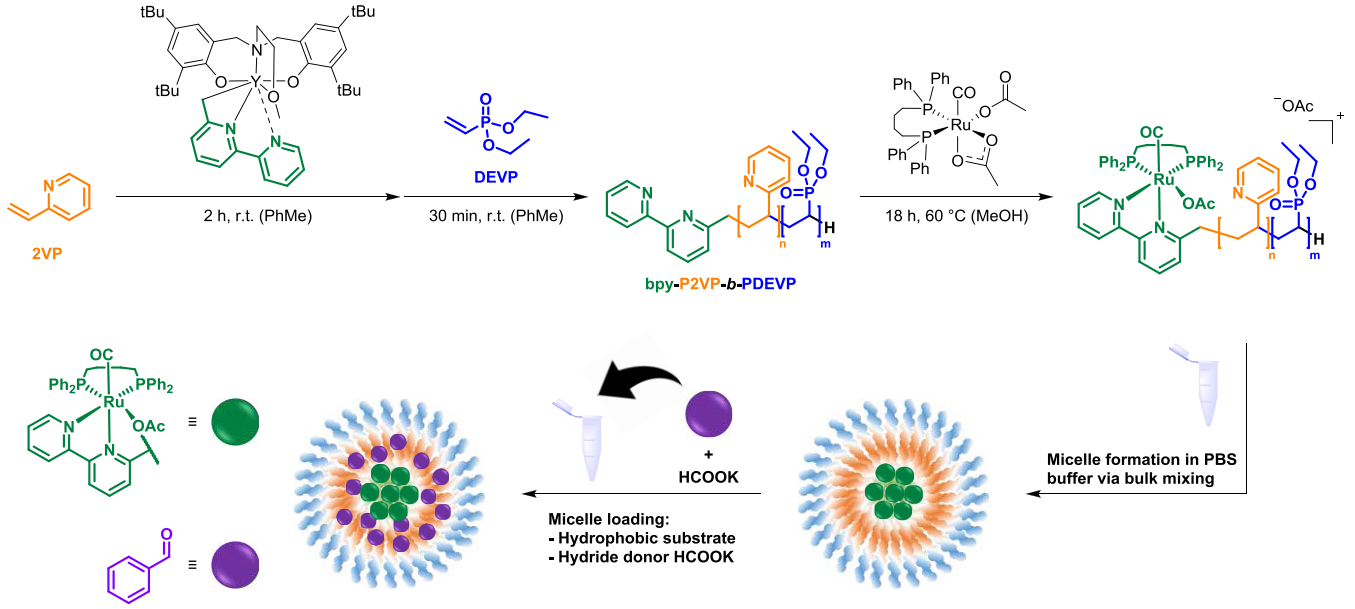

regeneration of the ruthenium-micelles showed retention of the catalytic performances for three consequent cycles.

RESULTS AND DISCUSSION

Polymer Synthesis and Functionalization. To establish an amphiphilic polymer scaffold for micellar transfer hydrogenation reactions of organic substrates, a strategy was applied whereby bipyridyl end-group-functionalized AB-type BCPs (bpy-P2VP-*b*-PDEVP) were synthesized and functionalized with a Ru(II) complex utilizing the bipyridyl moiety as a binding unit. Following the synthetic route for the monocarbonyl ruthenium precursor [Ru(η^1-OAc)(η^2-OAc)(dppb)-(CO)], the Ru(II) complex was tethered via coordination to the bipyridyl end-group of the polymer. The AB-type BCPs were synthesized using a yttrium bisphenolate catalyst bearing 6-methyl-2,2′-bipyridine as an initiating group via GTP (Scheme 1). This process benefited from controlled polymerization conditions and high initiation efficiencies.[29] The absolute molecular weight of the polymers was determined using the absolute molecular weight of P2VP and calculating the respective integrals from the ^{1}H NMR spectrum of the CH_2 group of PDEVP. However, due to the optimized SEC conditions, the polydispersity of BCPs was determined via SEC-MALS in THF/H_2O (Figures S1−S3).[37] The BCP character was confirmed by SEC in DMF and ^{1}H DOSY NMR studies (Figures S4−S13). Three polymers were obtained in different sizes (Table 1), namely, a small polymer (**SP**, 11.7 kg mol^{-1}), a medium-sized polymer (**MP**, 35.5 kg mol^{-1}), and a large polymer (**LP**, 81.7 kg mol^{-1}), respectively. The differently sized polymers were functionalized with the monocarbonyl ruthenium precursor [Ru(η^1-OAc)(η^2-OAc)-(dppb)(CO)] to yield [Ru(η^1-OAc)CO(dppb)(bpy-P2VP-*b*-PDEVP)]OAc in different sizes (small Ru polymer **SP**$_{[Ru]}$, medium Ru polymer **MP**$_{[Ru]}$, and large Ru polymer **LP**$_{[Ru]}$, Scheme 1), adapting a literature protocol.[2] Briefly, the ruthenium precursor was mixed in excess with the polymer and stirred in methanol at 60 °C under inert conditions. Methanol was removed *in vacuo*, and the crude product was dialyzed in water (MWCO 1 kDa) and purified via lyophilization, obtaining a light-yellowish polymer material.

A reactivity investigation was undertaken using simpler model substrates to evaluate the selectivity of the Ru(II) precursor toward N-donor groups within the polymer. The aim was to exclude competition from pyridyl groups of P2VP moieties in coordinating the metal. By utilization of the dppb ligand of the Ru(II) complex as a probe, the reactivity with model polymers was tracked by ^{31}P NMR spectroscopy. Owing to the low signal-to-noise ratio of dppb compared with the strong PDEVP signal in the ^{31}P NMR spectrum, detecting the Ru(II) complex was challenging. As a result, the reactivity study was conducted on simpler polymer substrates without PDEVP. To exclude binding or interaction with the P2VP motif, two model polymers, $SiMe_3$-P2VP (4.1 kg mol^{-1}) and bpy-P2VP (4.9 kg mol^{-1}), were synthesized following established procedures.[38] These polymers were then reacted with the [Ru(η^1-OAc)(η^2-OAc)(dppb)(CO)] precursor under the same conditions as those used for the functionalization of the AB-type BCPs with the Ru(II) complex (60 °C, MeOH, overnight, inert atmosphere, see Figure S14).[29,38] According to the obtained ^{31}P NMR spectra, $SiMe_3$-P2VP exhibited no significant interaction with [Ru(η^1-OAc)(η^2-OAc)(dppb)-(CO)] indicating inertness of the Ru(II) center toward the pyridyl groups of the P2VP motif. Instead, the reaction of bpy-P2VP with the precursor Ru(II) complex by means of the bpy end-group was promptly observed, as shown by the appearance of two doublets (δ = 31.0 and 29.0 ppm) in the ^{31}P NMR spectrum. These signals are similar to the chemical shifts of the recently published [RuCO(dppb)(bpy)(OAc)]OAc complex (δ = 31.2 and 29.2 ppm),[2] further proving the coordination of the Ru(II) center to the bipyridyl end-group of the polymer.

Micelle Formation and Characterization. Metal coordination to polymeric micelles can change the surfactant's aggregation properties and/or distribution of electrostatic charges and, therefore, induce a change in the aggregate's morphology. Therefore, to gain insights into the effects of Ru(II) complexation on the polymer's overall morphological and physicochemical properties, as well as on the arrangement

https://doi.org/10.1021/acsapm.4c02762
ACS Appl. Polym. Mater. 2024, 6, 13855−13864

Table 1. Synthesized Ru-Bipyridyl-Functionalized AB-Type BCPs of Different Sizes[a]

entry	DP A/B[b]	$M_{n,P2VP}$ [kg mol^{-1}][c]	$M_{n,AB}$ [kg mol^{-1}][b]	$Đ_{AB}$[d]	% [Ru][e]	ζ [mV][f]	TEM [nm]	D_h[g] [nm] pH 7.4	D_h[g] [nm] pH 6.3	D_h[g][nm] pH 5.4	CMC [mg mL^{-1}] pH 7.4	CMC [mg mL^{-1}] pH 5.4
SP	50:40	5.1	11.7	1.05	-	0.19 ± 0.12	no uniform micelle formation					
SP$_{[Ru]}$					65%	19.2 ± 1.4						
MP	150:120	16.3	35.5	1.05	-	−0.14 ± 0.49	29.1 ± 4.3	61.8 ± 0.1	60.0 ± 0.1	52.4 ± 0.4	0.08	0.09
MP$_{[Ru]}$					57%	6.55 ± 0.59	25.3 ± 10.2	63.6 ± 0.1	59.9 ± 0.2	55.5 ± 0.2	0.15	0.41
LP	340:280	35.7	81.7	1.15	-	−2.02 ± 0.02	60.3 ± 10.1	121 ± 0	119 ± 2	107 ± 1	0.08	0.09
LP$_{[Ru]}$					93%	−0.62 ± 0.41	56.6 ± 21.5	128 ± 1	136 ± 0	123 ± 0	0.21	0.48

[a]Physicochemical characterization of the obtained polymer compounds. [b]Absolute molecular weight and copolymer composition determined from the absolute molecular weight of P2VP and the aromatic signals versus OCH_3 phosphonate signals in ^{1}H NMR spectra (Figure S3). A = P2VP, B = PDEVP. [c]Absolute molecular weight (M_n) determination of P2VP via SEC in DMF. [d]Determination of polydispersity via SEC-MALS (THF/H_2O = (1:1), 9 g L^{-1} *tetra*-butyl ammonium bromide, 272 mg L^{-1} BHT). [e]Ruthenium content (%) determined by ICP-MS. [f]ζ-Potential determined via laser Doppler electrophoresis in ddH_2O. [g]Hydrodynamic diameter (D_h) determined via DLS in 100 mM PBS buffer at respective pH value.

of the Ru(II) moieties within the polymers' scaffold, the micelles were characterized in aqueous solution using different methods (Tables 1, S1, and S2). Bulk mixing of the purified Ru(II)-functionalized BCPs in 100 mM PBS buffer and pH values of 7.4 and 5.4 generates micelle solutions without the need for further filtration. Afterward, the ruthenium content in the micelles was quantified by inductively coupled plasma mass spectrometry (ICP-MS) analysis, which revealed, in all cases, a high degree (up to 93% for **LP**$_{[Ru]}$, Tables 1 and S2) of ruthenium functionalization with respect to the bipyridyl groups, depending on the polymer size.

The hydrodynamic diameter (D_h) of the micelles was determined *via* DLS in PBS buffer at different pH values. In the case of **LP**$_{[Ru]}$ and **MP**$_{[Ru]}$, uniform micelles could be observed at any investigated pH with an average D_h of 128 and 63.6 nm, respectively, indicating an apparent molecular weight (M_n) to size relationship (Tables 1 and S1, Figures S15 and S16). In contrast, **SP** and **SP**$_{[Ru]}$ fall below a particular molecular weight threshold and polymer composition, affecting the micelle formation so that no uniform micelle distribution could be observed (Figure S17, and Tables 1 and S1).[37] Comparing both larger Ru(II)-functionalized polymers with the nonfunctionalized ones, the size and micelle dispersities did not change significantly upon functionalization. ζ-Potential analysis conducted under buffered conditions was unsatisfactory due to the elevated salt concentration. Consequently, the determination of the ζ-potential was carried out in distilled deionized water (ddH_2O). In general, the ζ-potential values (Table 1) underwent significant changes with respect to the unfunctionalized micelles when the cationic Ru(II) complex was tethered at the polymer end-group. Specifically, while the **LP**$_{[Ru]}$ retained a slightly negative charge compared with the nonfunctionalized **LP**, **MP**$_{[Ru]}$ showed a markedly positive ζ-potential of +7 mV in ddH_2O (Figure 1A and Table 1). The slight negative surface charge of **LP**$_{[Ru]}$ indicates sufficient encapsulation of the ruthenium complex into the core of the micelle, providing a lipophilic environment of the catalytic center. In contrast, the cationic character of **MP**$_{[Ru]}$ indicates better accessibility of the positively charged ruthenium complexes toward the bulk aqueous phase. The small polymeric aggregates **SP**$_{[Ru]}$ showed the highest ζ-potential (+19 mV, Table 1), which comes along with the polydisperse shape observed in DLS (Figure S17), indicating randomly assembled polymers in solution. Both results prompted us to exclude **SP**$_{[Ru]}$ from further characterization. Complementary TEM images (Figure 1B−E) confirm the DLS results. The size distribution of **LP**$_{[Ru]}$ is narrow, with an average size of 57 nm, but shows structurally defined micelle networks with single micelles that are linked to larger structures. Similarly, **MP**$_{[Ru]}$ forms well-defined micelles of 25 nm size, fitting into the M_n-to-size relationship previously derived from DLS determination. In contrast to **LP**$_{[Ru]}$, the micelle network of **MP**$_{[Ru]}$ is not observed, while the individual shapes of the micelles are recognized as much sharper. In both cases, the observed size differences between TEM and DLS suggest a clear core−shell structure of the micelles.[39] Compared with the unfunctionalized BCPs (Figures S18 and S19), **LP**$_{[Ru]}$ and **MP**$_{[Ru]}$ (Figures 1B,D, S20, and S21) feature similar shape, size, and size distribution, corroborating the DLS results, showing a negligible impact of the Ru(II) functionalization on the overall micellar structure.

Under acidic conditions (pH 6.3 and 5.4), the apparent size distributions obtained via DLS increased, while the sizes

https://doi.org/10.1021/acsapm.4c02762
ACS Appl. Polym. Mater. 2024, 6, 13855−13864

slightly decreased (Table 1, and Figures S16 and S17). Both $\mathbf{MP}_{[Ru]}$ and $\mathbf{LP}_{[Ru]}$ showed an increased polydispersity as the P2VP units are partially protonated (buffering between pH 4 and 6), leading to higher repulsion forces within the former lipophilic micelle core.[40] Additional TEM images showed a complete change in the apparent shape of the micelles, exhibiting a less structured polymer distribution on the TEM grid (dark area, Figures S20 and S21). Within this area, the polymer forms bright spheres, indicating separated hydrophobic parts under these conditions. Comparing the results of the Ru(II)-functionalized with the unfunctionalized BCPs, the overall properties and the polymer behavior are similar.

However, the TEM images of $\mathbf{LP}_{[Ru]}$ at acidic pH value reveal a combination of dissolved polymer and intact micelles, suggesting a decrease in stability following the Ru(II) complex's functionalization due to the cationic charge (Figure S20).

The micellar characteristics were further investigated in solution for both functionalized and unfunctionalized BCPs. The critical micelle concentration (CMC) was determined in 100 mM PBS buffer (at pH 7.4 and 5.4) using a Nile red assay (Table 1).[41] The nonfunctionalized polymers (**LP** and **MP**) form micelles at 0.08 mg mL^{-1} CMC at pH 7.4. A similar CMC value is observed for pH 5.4 (0.09 mg mL^{-1}, Figure S22), indicating a minimal effect of the pH value on micelle formation. In contrast, both functionalized polymers ($\mathbf{LP}_{[Ru]}$ and $\mathbf{MP}_{[Ru]}$) exhibit increased CMCs of 0.2 mg mL^{-1} at pH 7.4, with an even higher CMC (0.4 mg mL^{-1}) at pH 5.4 (Figure S23). Introducing a cationic charge through the attached ruthenium complex reduces the micellar stability at low concentrations at pH 7.4, shifting the required amount of polymer for effective micellization to higher concentrations by a factor of 2. This effect is even more pronounced at an acidic pH value since the hydrophobic P2VP segments of the polymer are partly protonated (CMC higher by a factor of 4). Thereby, the hydrophilicity of the polymer is increased, reducing the thermodynamic sink, which is responsible for effective micellization. The conditions for certain applications to use such a micellar system must, therefore, be chosen at concentrations above the determined CMC.

To additionally prove the multiresponsive character of the micelles, their properties were characterized by DLS in PBS buffer (pH 7.4) at various temperatures ($\mathbf{LP}_{[Ru]}$, Figure 1F; **MP**, $\mathbf{M}_{[Ru]}$, **LP**, Figures S24 and S25). The results show a phase transition (lower critical solution temperature, LCST) for all micelles occurs at 33 °C, indicating size-independent properties. However, the reversibility of this transition is affected by the polymer composition. While both **LP** and $\mathbf{LP}_{[Ru]}$ show a high degree of reversibility in raising and lowering the temperature in the range of 20−50 °C, **MP** and $\mathbf{MP}_{[Ru]}$ do not reform evenly distributed and well-formed micelles when the temperature is decreased to the starting value.

Reduction of Biomass-Derived Aldehydes. Based on this extensive characterization, we selected the large Ru-BCP system $\mathbf{LP}_{[Ru]}$ for water-phase transfer hydrogenation reactions with different substrates. $\mathbf{LP}_{[Ru]}$ forms expansive micelles that entirely encapsulate the cationic Ru(II) moiety, creating a hydrophobic environment that is likely to enable the catalytic conversion of hydrophobic substrates in water. Additionally, the temperature-responsive behavior is reversible and enhances the potential of catalysis up to 30 °C. Thus, we focused our attention on poorly (or not at all) water-soluble biomass-derived aldehydes, such as benzaldehyde (**BA**), furfural (**FF**), 5-hydroxymethylfurfural (**HMF**), and 3,4-dimethoxybenzaldehyde (**MB**).[42] It is worth mentioning that among the methods developed for biomass valorization, reducing the oxygen content in biomass derivatives by hydrogenation or deoxidation is a key step toward valuable bioproducts and biofuels. These conversions can be performed using transfer hydrogenation metal catalysts or via eco-friendly photocatalytic processes, also applying noble metals or metal oxides.[43−45]

The catalytic efficiency of the Ru-micelles was compared in all cases to that of the free $[Ru(OAc)CO(dppb)(bpy)]^+$ complex (bpy = 2,2′-bipyridine). The reduction of the substrates was monitored by ^1H NMR spectroscopy using potassium formate as a hydride source in deuterated PBS at a neutral pH (7.4). Buffered conditions were chosen since BCPs form a pH-responsive material. The temperature of the catalysis (30 °C) was chosen to be below the determined LCST of 33 °C (Figure 1F). The molar ratio of both [Ru(bpy)] and $\mathbf{LP}_{[Ru]}$ was kept constant (0.24 mM), as well as the concentration of the reducing agent (72 mM), while the concentration of the substrates was varied (12, 30, and 48 mM) (see Experimental Section for details). For **MB** and **BA** substrates, additional catalysis experiments were performed at lower concentrations of 2.4 and 6 mM, respectively. It has to be noted that the concentration of $\mathbf{LP}_{[Ru]}$ used for the transfer hydrogenation studies (20 mg mL^{-1}) is more than 90-fold higher than the measured CMC value at pH 7.4 (see the previous section) to achieve the same Ru catalyst concentration used in the previous work.[2] We assume that also in this case, $\mathbf{LP}_{[Ru]}$ reacts with formate to afford the hydride derivative of the ruthenium micelle ($\mathbf{LP}_{[Ru-H]}$) via β-hydride elimination accompanied by CO_2 evolution. The micelle can then hydrogenate the aldehyde substrates to alcohols while regenerating $\mathbf{LP}_{[Ru-H]}$ (Figure 2A). Representative ^1H NMR spectra are reported in Figure 2B for the reduction of benzaldehyde, while the trends of the turnover numbers vs time at pH 7.4 for the reduction of **MB**, **BA**, **FF**, and **HMF** are reported in the Supporting Information (Figures S26−S32). According to the obtained results, the catalytic activity of $\mathbf{LP}_{[Ru]}$ toward aldehydes showed a marked dependence on the solubility of such substrates in water. In detail, the rate of the transfer hydrogenation increased with the lipophilic character of the substrates in the order **MB** > **BA** > **FF** > **HMF**, being **MB** ($\log P$ = 1.64) reduced *ca.* 6-fold faster than the most hydrophilic substrate **HMF** ($\log P$ = −0.78), the latter not even reaching complete conversion (Figure 2C and Table 2).[46] TOF numbers in the range of 50% conversion were calculated. The ruthenium micelle itself was not able to perform any catalytic conversion toward the studied substrates in the absence of formate as the reducing agent. Of note, complex [RuCO(dppb)(bpy)(OAc)]OAc showed no TH ability toward any of the selected substrates, pointing out the relevance of the micellar system in the observed catalytic activity.

Furthermore, we observed a strong direct dependence of the TOF numbers on the substrate concentrations while keeping the other parameters constant (Figure 2C). Thus, upon increased aldehyde concentrations from 12 to 48 mM, TOF numbers reached values as high as 20 h^{-1} for **MB** (Table 2). Conversely, **HMF**, being moderately water soluble, exhibits slower conversion to the corresponding alcohol, never reaching complete conversion in 48 h (80% conversion for 48 mM **HMF** solution). It should be noted that the plot of the TOF

https://doi.org/10.1021/acsapm.4c02762
ACS Appl. Polym. Mater. 2024, 6, 13855−13864

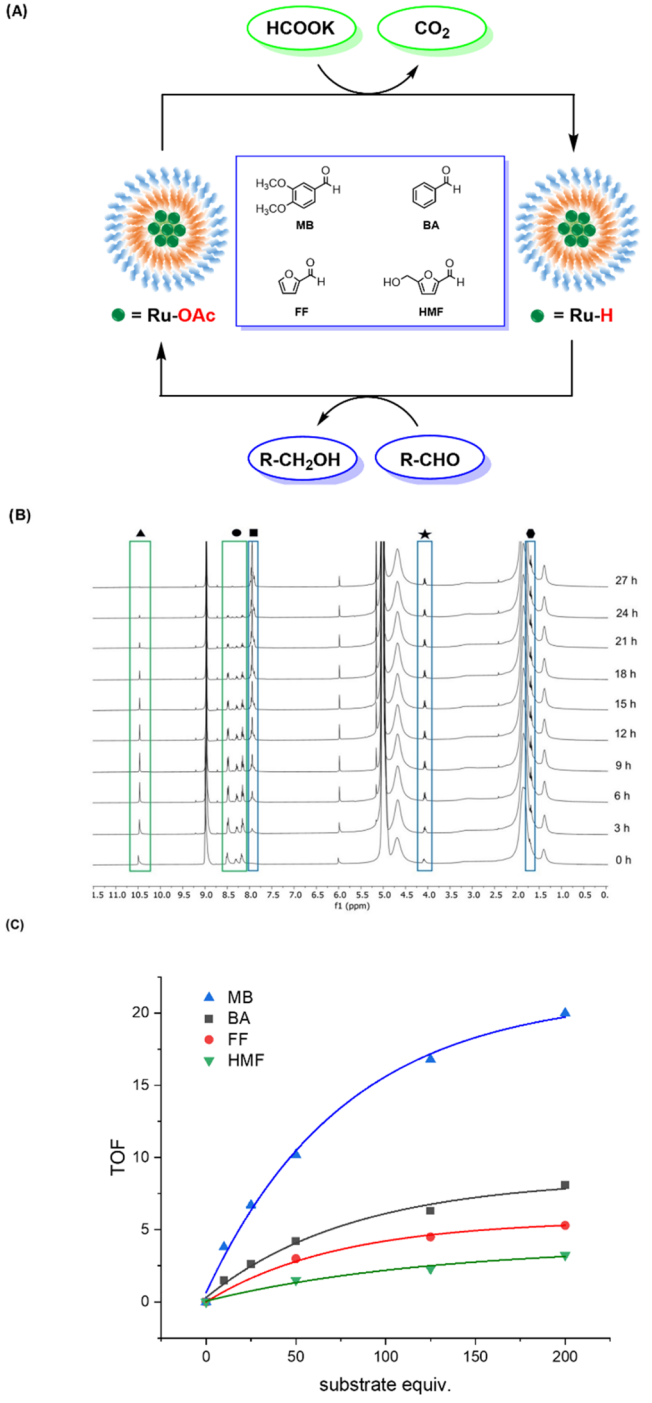

Figure 2. (A) Proposed catalytic pathway for the reduction of 3,4-dimethoxybenzaldehyde (**MB**), benzaldehyde (**BA**), furfural (**FF**), and 5-hydroxymethylfurfural (**HMF**) accomplished by $\mathbf{LP}_{[Ru]}$ in PBS buffer (pH 7.4). (B) Stacked ^{1}H NMR kinetics of the reduction of benzaldehyde performed by $\mathbf{LP}_{[Ru]}$, showing the formation of benzyl alcohol (in deuterated PBS buffer at pH 7.4 over 27 h with molar ratios of $LP_{[Ru]}$/BA/HCOOK = 1:200:300). The benzaldehyde resonances into the green boxes are represented by the aldehyde proton (triangle) and the aromatic protons (circle), while the formed benzyl alcohol provides new signals highlighted into the blue boxes for the aromatic protons (square), the CH_2 protons (star), and finally the OH proton (hexagon). (C) Plot of the turnover frequency (TOF, moles of aldehyde converted to alcohol per mole of the catalyst per hour), for $\mathbf{LP}_{[Ru]}$ (0.24 mM) against substrate equivalents (0, 50, 125, and 200 for **HMF** and **FF**; 0, 10, 25, 50, 125, and 200 for **MB** and **BA**), keeping $LP_{[Ru]}$/HCOOK constant (1:300) at pH 7.4.

numbers over the aldehyde concentrations shows a nonlinear trend, reaching a plateau at higher substrate concentrations (Figure 2C).

Decreasing the pH to 5.4, the catalytic performances of the Ru-micelles are quantitatively lost (Figure S33A), likely due to the protonation of the micelles at the hydrophobic P2VP site (Figure S33B), leading to an increased repulsion of the polymer and the hydrophobic substrate. This assumption is also in line with the DLS experiments (see the previous section), showing more aggregate micellar species at lower pH.

With regard to the stability of the micelles during catalysis, DLS of $\mathbf{LP}_{[Ru]}$ was measured exemplarily for the reactions of benzaldehyde and furfural prior to and right after catalysis (Figure 3A). The micellar character was retained for both substrates, which was further confirmed by ^{1}H NMR experiments (Figure S34). Relying on the striking stability of the micelles after performing transfer hydrogenation reactions toward the previously mentioned aldehydes, the reaction solution was dialyzed, and the micelles were regenerated by dialysis against water and lyophilized and employed again for three more catalytic cycles toward benzaldehyde reduction (2.4 mM). After two catalytic cycles, the micellar systems showed retention of the catalytic performances (TOF ca. 2 h^{-1}, 98–100% conversion within 5 h), while during the third and fourth cycles, the catalytic performances went gradually lost, reaching 50% conversion of benzaldehyde in 5 h (Figure 3B). The DLS analysis of the micelles after the fourth cycle of catalysis with BA showed only a slight broadening of the size distribution by maintaining the size (Z-average) of the micelles. Therefore, the loss of catalytic activity is most likely due to the deactivation of the ruthenium catalyst in water and under air conditions. Indeed, it has been shown that diphosphine ligands can be prone to oxidation under such conditions, leading to the loss of catalytic activity over time.[47]

CONCLUSIONS

In conclusion, we describe here the synthesis of a ruthenium-functionalized AB-type BCP obtained via coordination of the ruthenium fragment [Ru(η^1-OAc)(dppb)(CO)] to the bipyridine end-group of the polymer. Three polymers were obtained of different sizes. Following a straightforward two-step synthesis protocol to obtain the Ru(II)-functionalized polymer, the catalytically active micelles are fabricated by simple bulk mixing in PBS buffer at various pH values. The physicochemical characterization by DLS and TEM oriented the choice of the larger polymeric micelles as the most suitable to catalyze TH of hydrophobic aldehydes in water, expanding the substrate scope compared with the previous studies.[2] The obtained results show that the Ru-micelles can catalyze the reduction of aldehydes in buffered aqueous solution (pH 7.4) at 30 °C in the presence of formate. Of note, the free Ru(II) complex is not active on the same substrates and experimental conditions. Moreover, the micelles can be regenerated up to three times, preserving good catalytic activity.

The catalytic mechanism of TH of the Ru-micelles with the selected hydrophobic substrates should be further investigated by different methods, including density functional theory (DFT) calculations. Nevertheless, preliminary studies have shown that in the catalytic NAD^+ hydrogenation with formate as the H-donor, the rate-limiting step is the transfer of the ruthenium hydride to the NAD^+ substrate.[2] Instead, NADH oxidation by the Ru(II) monocarbonyl complex sees the H-transfer from 1,4-NADH as the rate-limiting step.

https://doi.org/10.1021/acsapm.4c02762
ACS Appl. Polym. Mater. 2024, 6, 13855–13864

Table 2. Catalytic Activity for the Reduction of 3,4-Dimethoxybenzaldehyde (MB), Benzaldehyde (BA), Furfural (FF), and 5-Hydroxymethylfurfural (HMF) Catalysed by $LP_{[Ru]}$ and [Ru(bpy)] in PBS (pH 7.4 and 5.5) at 30 °C, Where [cat]/[Aldehyde]/[HCOOK] = 0.24 mM:*X*:72 mM (*X* = 12, 30, or 48 mM) Corresponding to Molar Ratios of 1:*X*:300 (*X* = 50, 125, 200)[a]

		TOF (h^{-1})											
catalyst		MB 3,4-dimethoxybenzaldehyde			BA benzaldehyde			FF furfural			HMF 5-Hydroxymethylfurfural		
		12 mM	30 mM	48 mM	12 mM	30 mM	48 mM	12 mM	30 mM	48 mM	12 mM	30 mM	48 mM
$LP_{[Ru]}$	pH 7.4	9.9	15.7	20.0	4.0	6.3	8.1	3.0	4.5	5.3	1.5	2.3	3.2
	pH 5.5	0.4	-	-	0.5	-	-	0.7	-	-	0.8	-	-

[a]TOF refers to the turnover per unit time and is expressed as the number of moles of consumed aldehyde per mole of catalyst after 1 h.

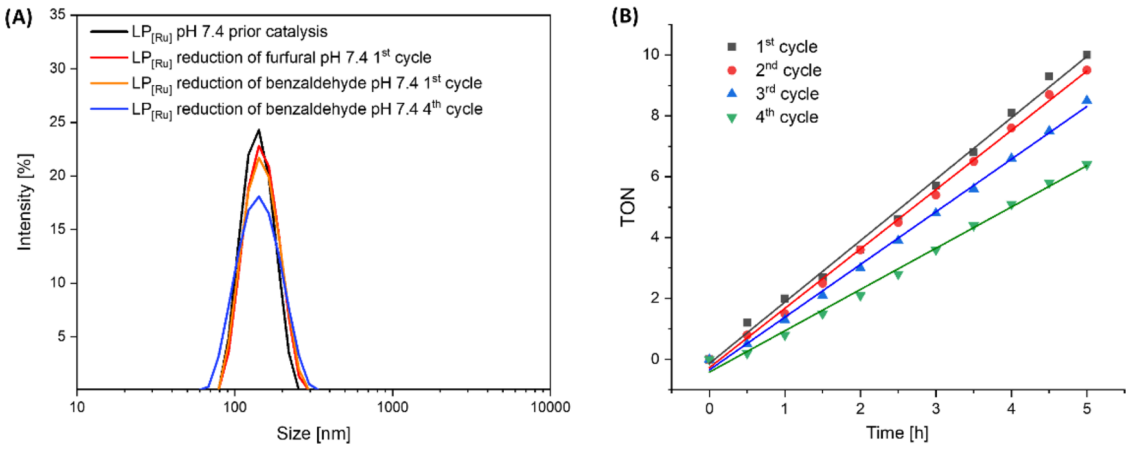

Figure 3. (A) DLS determination of $LP_{[Ru]}$ before and after conversion of furfural (1st cycle) and benzaldehyde (1st and 4th cycles) at 1 mg mL^{-1}. (B) Trends of conversion (TON) vs time with molar ratios of $[LP_{[Ru]}]$/[BA]/[HCOOK] = 1:10:300 at acidic pH = 7.4. The micelles were regenerated for three additional catalytic cycles.

Having the ruthenium catalyst encapsulated into micellar systems surely opens the door toward unprecedented forms of reactivity exploiting the different interactions between micelles and substrates and could be extended to other monocarbonyl Ru(II) derivatives.[5,6] Ongoing studies in our group are devoted to the integration of more active and selective Ru(II) catalysis into the BCP-micellar systems to achieve TH of different organic substrates, including for regeneration of 1,4-NADH. The latter is an essential cofactor for oxidoreductases (dehydrogenases) in biochemical reactions, but is also used in the industrial preparation of organic compounds. Therefore, the Ru(II) micelles can be used for the synthesis of many industrially relevant compounds, or as "therapeutic" catalysts in cells.[48,49] In this case, the presence of the micelle would favor the metallodrug delivery at the tumor site and the uptake of the Ru(II) catalyst into cancer cells.

EXPERIMENTAL SECTION

General. All reactions were carried out under an argon atmosphere using standard Schlenk techniques. All glassware were heat-dried under a vacuum before use. Polymerizations with moisture- and air-sensitive reactants were carried out in an MBraun LabMaster120 glovebox filled with argon 4.6 from Westfalen or using standard Schlenk techniques. Unless otherwise stated, all chemicals were purchased from Sigma-Aldrich or TCI and used without further purification. Toluene, pentane, and THF for polymerization reactions were dried using an MBraun SPS-800 solvent purification system and stored over 3 Å molecular sieves. The starting materials for the complex synthesis of $LiCH_2TMS$,[50] bisphenolate ligand $[ONOO]^{tBu}$,[51] 6-methyl-2,2′-bipyridine,[52] the complex $[ONOO]^{tBu}Y(CH_2TMS)(thf)$,[53] and $[ONOO]^{tBu}Y(6\text{-Mebpy})(thf)$[29] (**Y**) were prepared according to literature procedures. Diethyl vinylphosphonate (DEVP)[54] was synthesized according to the procedures in the literature, dried over calcium hydride, and distilled prior to use. 2-Vinylpyridine (2VP) was dried over calcium hydride and distilled prior to use. The synthesis of ruthenium precursor $[Ru(\eta^1\text{-OAc})(\eta^2\text{-OAc})CO(dppb)]$[55] was achieved according to previously established procedures.

General Polymerization Procedure. $[ONOO]^{tBu}Y(6\text{-Mebpy})$ (57.0 mg, 74.3 μmol, 1.00 equiv) was dissolved in 22 mL of PhMe, and the calculated amount of 2VP was added to the reaction mixture under continuous stirring. After 2 h, an aliquot was taken from the reaction mixture, and the conversion was determined by ^1H NMR. Afterward, the calculated amount of DEVP was added to the reaction mixture. After 1 h, an aliquot was taken from the reaction mixture, and the conversion was determined by ^{31}P NMR spectroscopy. The polymerization was quenched with 0.5 mL of ethanol, and the mixture was precipitated from pentane (40 mL), centrifugated, and decanted. The polymer was lyophilized from 1,4-dioxane and obtained as a white solid.

General Procedure for the Polymer Ruthenium Functionalization. To a solution of polymer in MeOH, the ruthenium precursor $[Ru(\eta^1\text{-OAc})\text{-}(\eta^2OAc)(dppb)(CO)]$ (4 equiv) was added under continuous stirring. The reaction mixture was heated to 65 °C and stirred under a nitrogen atmosphere. The solvent was removed under reduced pressure. The crude was dissolved in ddH_2O and purified via dialysis (MWCO 1 kDa) and lyophilized to obtain purified ruthenium-functionalized polymers $\mathbf{P}_{[Ru]}$ as a yellowish fluffy solid.

Micelles Fabrication. The purified functionalized polymers were dissolved at the desired concentrations at room temperature in 100 mM PBS buffer at pH 7.4 and 5.4, respectively, and used without filtration or further purification. The stock solutions were stored at 4 °C.

Catalytic Activity Determinations. 3,4-Dimethoxybenzaldehyde (**MB**), benzaldehyde (**BA**), furfural (**FF**), and 5-hydroxymethylfurfural (**HMF**) reduction was performed reacting $\mathbf{LP}_{[Ru]}$ or [Ru(OAc)-

https://doi.org/10.1021/acsapm.4c02762
ACS Appl. Polym. Mater. 2024, 6, 13855−13864

CO(dppb)(bpy)]OAc (0.24 mM) with the examined aforementioned substrates at different concentrations (12, 30, or 48 mM) in PBS at pD 5.5 and 7.4. MB and BA substrates were additionally tested in concentrations of 2.4 and 6 mM. Before starting the ^{1}H NMR kinetics, 300 equiv of potassium formate were added to the solution (to achieve a concentration of 272 mM) and 0.5 mL of the solution was transferred into a 5 mm NMR tube. ^{1}H NMR spectra were recorded every 30 min up to 24 h and every hour until 48 h at 30 °C.

Micelles Regeneration. The reaction solution after catalysis was purified via dialysis (MWCO 1 kDa) for 24 h and lyophilized to recover the pure ruthenium-functionalized polymers $\mathbf{LP}_{[Ru]}$ as a fluffy solid, which was then reused in a second catalytic cycle toward the reduction of benzaldehyde (2.4 mM). The micellar system was regenerated and applied in catalysis two more times following the abovementioned procedure. The experiment was repeated twice.

■ ASSOCIATED CONTENT

Supporting Information

The Supporting Information is available free of charge at https://pubs.acs.org/doi/10.1021/acsapm.4c02762.

A detailed Experimental Section and the characterization of the micelles by different methods, as well as their catalytic activity (Figures S1−S34 and Tables S1 and S2) (PDF)

■ AUTHOR INFORMATION

Corresponding Authors

Bernhard Rieger − *WACKER-Chair of Macromolecular Chemistry, Catalysis Research Center, School of Natural Sciences, Technical University of Munich, D-85748 Garching b. München, Germany;* orcid.org/0000-0002-0023-884X; Email: rieger@tum.de

Angela Casini − *Chair of Medicinal and Bioinorganic Chemistry, Department of Chemistry, School of Natural Sciences, Technical University of Munich, D-85748 Garching b. München, Germany;* orcid.org/0000-0003-1599-9542; Email: angela.casini@tum.de

Authors

Denise Lovison − *Chair of Medicinal and Bioinorganic Chemistry, Department of Chemistry, School of Natural Sciences, Technical University of Munich, D-85748 Garching b. München, Germany*

Philipp Weingarten − *WACKER-Chair of Macromolecular Chemistry, Catalysis Research Center, School of Natural Sciences, Technical University of Munich, D-85748 Garching b. München, Germany*

Alexandra Sebeschuk − *Chair of Medicinal and Bioinorganic Chemistry, Department of Chemistry, School of Natural Sciences, Technical University of Munich, D-85748 Garching b. München, Germany*

Complete contact information is available at: https://pubs.acs.org/10.1021/acsapm.4c02762

Author Contributions

§D.L. and P.W. contributed equally to this work.

Notes

The authors declare no competing financial interest.

■ ACKNOWLEDGMENTS

The authors acknowledge the support from the TUM Innovation Network "Artificial Intelligence Powered Multi-functional Material Design" (ARTEMIS).

■ REFERENCES

(1) Rideout, D. C.; Breslow, R. Hydrophobic acceleration of Diels-Alder reactions. *J. Am. Chem. Soc.* **1980**, *102* (26), 7816−7817.

(2) Lovison, D.; Berghausen, T.; Thomas, S. R.; Robson, J.; Drees, M.; Jandl, C.; Pöthig, A.; Mollik, P.; Halter, D. P.; Baratta, W.; Casini, A. Beyond Metal-Arenes: Monocarbonyl Ruthenium(II) Catalysts for Transfer Hydrogenation Reactions in Water and in Cells. *ACS Catal.* **2023**, *13* (16), 10798−10823.

(3) Lovison, D.; Alessi, D.; Allegri, L.; Baldan, F.; Ballico, M.; Damante, G.; Galasso, M.; Guardavaccaro, D.; Ruggieri, S.; Melchior, A.; Veclani, D.; Nardon, C.; Baratta, W. Enantioselective Cytotoxicity of Chiral Diphosphine Ruthenium(II) Complexes Against Cancer Cells. *Chem. - Eur. J.* **2022**, *28* (33), No. e202200200.

(4) Lovison, D.; Allegri, L.; Baldan, F.; Ballico, M.; Damante, G.; Jandl, C.; Baratta, W. Cationic carboxylate and thioacetate ruthenium-(ii) complexes: synthesis and cytotoxic activity against anaplastic thyroid cancer cells. *Dalton Trans.* **2020**, *49* (24), 8375−8388.

(5) Figliolia, R.; Cavigli, P.; Comuzzi, C.; Del Zotto, A.; Lovison, D.; Strazzolini, P.; Susmel, S.; Zuccaccia, D.; Ballico, M.; Baratta, W. CNN pincer ruthenium complexes for efficient transfer hydrogenation of biomass-derived carbonyl compounds. *Dalton Trans.* **2020**, *49* (2), 453−465.

(6) Baldino, S.; Giboulot, S.; Lovison, D.; Nedden, H. G.; Pöthig, A.; Zanotti-Gerosa, A.; Zuccaccia, D.; Ballico, M.; Baratta, W. Preparation of Neutral trans - cis Ru(O2CR)2P2(NN), Cationic Ru(O2CR)P2-(NN)(O2CR) and Pincer Ru(O2CR)(CNN)P2 (P = PPh3, P2 = diphosphine) Carboxylate Complexes and their Application in the Catalytic Carbonyl Compounds Reduction. *Organometallics* **2021**, *40* (8), 1086−1103.

(7) La Sorella, G.; Strukul, G.; Scarso, A. Recent advances in catalysis in micellar media. *Green Chem.* **2015**, *17* (2), 644−683.

(8) Lorenzetto, T.; Frigatti, D.; Fabris, F.; Scarso, A. Nanoconfinement Effects of Micellar Media in Asymmetric Catalysis. *Adv. Synth. Catal.* **2022**, *364* (11), 1776−1797.

(9) Scarso, A. Micellar Nanoreactors. In *Encyclopedia of Inorganic and Bioinorganic Chemistry*; Scott, R. A., Ed.; Wiley, 2012; pp 1−16.

(10) Brüss, L.; Jeyaseelan, R.; Kürschner, J. C. G.; Utikal, M.; Næsborg, L. Micellar Effects and their Relevance in Photochemistry and Photocatalysis. *ChemCatChem* **2023**, *15* (1), No. e202201146.

(11) Nicolai, T.; Colombani, O.; Chassenieux, C. Dynamic polymeric micelles versus frozen nanoparticles formed by block copolymers. *Soft Matter* **2010**, *6* (14), 3111−3118.

(12) Qu, P.; Kuepfert, M.; Ahmed, E.; Liu, F.; Weck, M. Cross-Linked Polymeric Micelles as Catalytic Nanoreactors. *Eur. J. Inorg. Chem.* **2021**, *2021* (15), 1420−1427.

(13) Bortenschlager, M.; Schöllhorn, N.; Wittmann, A.; Weberskirch, R. Triphenylphosphane-functionalised amphiphilic copolymers: tailor-made support materials for the efficient and selective aqueous two-phase hydroformylation of 1-octene. *Chem. - Eur. J.* **2007**, *13* (2), 520−528.

(14) Huerta, E.; Stals, P. J. M.; Meijer, E. W.; Palmans, A. R. A. Consequences of folding a water-soluble polymer around an organocatalyst. *Angew. Chem., Int. Ed.* **2013**, *52* (10), 2906−2910.

(15) Lempke, L.; Ernst, A.; Kahl, F.; Weberskirch, R.; Krause, N. Sustainable Micellar Gold Catalysis − Poly(2-oxazolines) as Versatile Amphiphiles. *Adv. Synth. Catal.* **2016**, *358* (9), 1491−1499.

(16) Lu, J.; Dimroth, J.; Weck, M. Compartmentalization of Incompatible Catalytic Transformations for Tandem Catalysis. *J. Am. Chem. Soc.* **2015**, *137* (40), 12984−12989.

(17) Nghiem, T.-L.; Coban, D.; Tjaberings, S.; Gröschel, A. H. Recent Advances in the Synthesis and Application of Polymer Compartments for Catalysis. *Polymers* **2020**, *12* (10), No. 2190.

(18) Schönfelder, D.; Nuyken, O.; Weberskirch, R. Heck and Suzuki coupling reactions in water using poly(2-oxazoline)s functionalized with palladium carbene complexes as soluble, amphiphilic polymer supports. *J. Organomet. Chem.* **2005**, *690* (21−22), 4648−4655.

(19) Schoonen, L.; van Hest, J. C. M. Compartmentalization Approaches in Soft Matter Science: From Nanoreactor Development to Organelle Mimics. *Adv. Mater.* **2016**, *28* (6), 1109−1128.

(20) Uozumi, Y.; Kimura, T. Heck Reaction in Water with Amphiphilic Resin-Supported Palladium-Phosphine Complexes. *Synlett* **2002**, No. 12, 2045−2048.
(21) van Dongen, S. F. M.; de Hoog, H.-P. M.; Peters, R. J. R. W.; Nallani, M.; Nolte, R. J. M.; van Hest, J. C. M. Biohybrid polymer capsules. *Chem. Rev.* **2009**, *109* (11), 6212−6274.
(22) Lin, Z.; Li, J.; Huang, Q.; Huang, Q.; Wang, Q.; Tang, L.; Gong, D.; Yang, J.; Zhu, J.; Deng, J. Chiral surfactant-type catalyst: enantioselective reduction of long-chain aliphatic ketoesters in water. *J. Org. Chem.* **2015**, *80* (9), 4419−4429.
(23) Li, J.; Tang, Y.; Wang, Q.; Li, X.; Cun, L.; Zhang, X.; Zhu, J.; Li, L.; Deng, J. Chiral surfactant-type catalyst for asymmetric reduction of aliphatic ketones in water. *J. Am. Chem. Soc.* **2012**, *134* (45), 18522−18525.
(24) Qu, P.; Cleveland, J. W.; Ahmed, E.; Liu, F.; Dubrawski, S.; Jones, C. W.; Weck, M. Compartmentalisation of molecular catalysts for nonorthogonal tandem catalysis. *Chem. Soc. Rev.* **2022**, *51* (1), 57−70.
(25) Liu, F.; Qu, P.; Weck, M. Photoresponsive Azobenzene-Functionalized Shell Cross-Linked Micelles for Selective Asymmetric Transfer Hydrogenation. *Org. Lett.* **2022**, *24* (23), 4099−4103.
(26) Zhou, L.; Ji, P.; Wang, X.; Qi, D.; Chen, T. Polymeric Micelles with Chiral Diamine-Ru(II) Catalysts for Asymmetric Transfer Hydrogenation of Ketones in Water. *J. Inorg. Organomet. Polym. Mater.* **2024**, *34* (3), 1172−1180.
(27) Öztürk, B. Ö.; Öztürk, S. Transfer-hydrogenation reactions of ketones/aldehydes in water using first generation ruthenium indenylidene olefin metathesis catalyst: One step towards sequential cross-metathesis/transfer hydrogenation reactions. *Mol. Catal.* **2020**, *480*, No. 110640.
(28) Joumaa, A.; Chen, S.; Vincendeau, S.; Gayet, F.; Poli, R.; Manoury, E. Rhodium-catalyzed aqueous biphasic hydrogenation of alkenes with amphiphilic phosphine-containing core-shell polymers. *Mol. Catal.* **2017**, *438*, 267−271.
(29) Adams, F.; Pschenitza, M.; Rieger, B. Yttrium-Catalyzed Synthesis of Bipyridine-Functionalized AB-Block Copolymers: Micellar Support for Photocatalytic Active Rhenium-Complexes. *ChemCatChem* **2018**, *10* (19), 4309−4316.
(30) Schwarzenböck, C.; Schaffer, A.; Pahl, P.; Nelson, P. J.; Huss, R.; Rieger, B. Precise synthesis of thermoresponsive polyvinylphosphonate-biomolecule conjugates via thiol−ene click chemistry. *Polym. Chem.* **2018**, *9* (3), 284−290.
(31) Pahl, P.; Schwarzenböck, C.; Herz, F. A. D.; Soller, B. S.; Jandl, C.; Rieger, B. Core-First Synthesis of Three-Armed Star-Shaped Polymers by Rare Earth Metal-Mediated Group Transfer Polymerization. *Macromolecules* **2017**, *50* (17), 6569−6576.
(32) Altenbuchner, P. T.; Werz, P. D. L.; Schöppner, P.; Adams, F.; Kronast, A.; Schwarzenböck, C.; Pöthig, A.; Jandl, C.; Haslbeck, M.; Rieger, B. Next Generation Multiresponsive Nanocarriers for Targeted Drug Delivery to Cancer Cells. *Chem. - Eur. J.* **2016**, *22* (41), 14576−14584.
(33) Adams, F.; Pahl, P.; Rieger, B. Metal-Catalyzed Group-Transfer Polymerization: A Versatile Tool for Tailor-Made Functional (Co)Polymers. *Chem. - Eur. J.* **2018**, *24* (3), 509−518.
(34) Schaffer, A.; Kränzlein, M.; Rieger, B. Precise Synthesis of Poly(dimethylsiloxane) Copolymers through C−H Bond-Activated Macroinitiators via Yttrium-Mediated Group Transfer Polymerization and Ring-Opening Polymerization. *Macromolecules* **2020**, *53* (19), 8382−8392.
(35) Kränzlein, M.; Pehl, T. M.; Halama, K.; Großmann, P. F.; Kratky, T.; Mühlbach, A. M.; Rieger, B. Azide-Modified Poly(diethyl vinylphosphonate) for Straightforward Graft-to Carbon Nanotube Functionalization. *Macromol. Mater. Eng.* **2023**, *308* (6), No. 2200635.
(36) Weingarten, P.; Thomas, S. R.; de Andrade Querino, A. L.; Halama, K.; Kränzlein, M.; Casini, A.; Rieger, B. A graft-to strategy of poly(vinylphosphonates) on dopazide-coated gold nanoparticles using in situ catalyst activation. *RSC Adv.* **2024**, *14* (12), 8145−8149.
(37) Adams, F.; Altenbuchner, P. T.; Werz, P. D. L.; Rieger, B. Multiresponsive micellar block copolymers from 2-vinylpyridine and dialkylvinylphosphonates with a tunable lower critical solution temperature. *RSC Adv.* **2016**, *6* (82), 78750−78754.
(38) Adams, F.; Machat, M. R.; Altenbuchner, P. T.; Ehrmaier, J.; Pöthig, A.; Karsili, T. N. V.; Rieger, B. Toolbox of Nonmetallocene Lanthanides: Multifunctional Catalysts in Group-Transfer Polymerization. *Inorg. Chem.* **2017**, *56* (16), 9754−9764.
(39) Wilson, B. K.; Prud'homme, R. K. Nanoparticle size distribution quantification from transmission electron microscopy (TEM) of ruthenium tetroxide stained polymeric nanoparticles. *J. Colloid Interface Sci.* **2021**, *604*, 208−220.
(40) Atanase, L. I.; Riess, G. Micellization of pH-stimulable poly(2-vinylpyridine)-b-poly(ethylene oxide) copolymers and their complexation with anionic surfactants. *J. Colloid Interface Sci.* **2013**, *395*, 190−197.
(41) Peterson, A. M.; Tan, Z.; Kimbrough, E. M.; Heemstra, J. M. 3,3′-Dioctadecyloxacarbocyanine perchlorate (DiO) as a fluorogenic probe for measurement of critical micelle concentration. *Anal. Methods* **2015**, *7* (16), 6877−6882.
(42) Nakagawa, Y.; Tamura, M.; Tomishige, K. Catalytic Reduction of Biomass-Derived Furanic Compounds with Hydrogen. *ACS Catal.* **2013**, *3* (12), 2655−2668.
(43) Meng, Y.; Jian, Y.; Li, J.; Wu, H.; Zhang, H.; Saravanamurugan, S.; Yang, S.; Li, H. Surface-active site engineering: Synergy of photo- and supermolecular catalysis in hydrogen transfer enables biomass upgrading and H2 evolution. *Chem. Eng. J.* **2023**, *452*, No. 139477.
(44) Jian, Y.; Meng, Y.; Li, J.; Wu, H.; Saravanamurugan, S.; Li, H. Engineering oxygen vacancy and crystal surfaces for TiO2-based photocatalysts for enhanced photocatalytic hydrogenation of bio-based carbonyls to biofuels. *J. Environ. Chem. Eng.* **2022**, *10* (6), No. 108837.
(45) Gilkey, M. J.; Xu, B. Heterogeneous Catalytic Transfer Hydrogenation as an Effective Pathway in Biomass Upgrading. *ACS Catal.* **2016**, *6* (3), 1420−1436.
(46) Tetko, I. V.; Gasteiger, J.; Todeschini, R.; Mauri, A.; Livingstone, D.; Ertl, P.; Palyulin, V. A.; Radchenko, E. V.; Zefirov, N. S.; Makarenko, A. S.; Tanchuk, V. Y.; Prokopenko, V. V. Virtual computational chemistry laboratory–design and description. *J. Comput.-Aided Mol. Des.* **2005**, *19* (6), 453−463.
(47) Horký, F.; Franz, R.; Bruhn, C.; Pietschnig, R. A General Strategy for Increasing the Air Stability of Phosphines Including Primary Phosphines. *Chem. - Eur. J.* **2023**, *29* (68), No. e202302518.
(48) Trotta, C.; Rodriguez, G. M.; Zuccaccia, C.; Macchioni, A. Electrochemical NADH Regeneration Mediated by Pyridine Amidate Iridium Complexes Interconverting 1,4- and 1,6-NADH. *ACS Catal.* **2024**, *14* (13), 10334−10343.
(49) Ma, S. K.; Gruber, J.; Davis, C.; Newman, L.; Gray, D.; Wang, A.; Grate, J.; Huisman, G. W.; Sheldon, R. A. A green-by-design biocatalytic process for atorvastatin intermediate. *Green Chem.* **2010**, *12* (1), 81−86.
(50) Vaughn, G. D.; Krein, A. K.; Gladysz, J. A. Synthesis and reactivity of metallacyclic manganese. alpha.-(silyloxy)alkyl complexes [cyclic] (CO)4MnC(R)(OSi(CH3)3)P(C6H5)2. A new thermodynamic driving force for carbonyl insertion. *Organometallics* **1986**, *5* (5), 936−942.
(51) Tshuva, E. Y.; Groysman, S.; Goldberg, I.; Kol, M.; Goldschmidt, Z. [ONXO]-Type Amine Bis(phenolate) Zirconium and Hafnium Complexes as Extremely Active 1-Hexene Polymerization Catalysts. *Organometallics* **2002**, *21* (4), 662−670.
(52) Rayder, T. M.; Adillon, E. H.; Byers, J. A.; Tsung, C.-K. A Bioinspired Multicomponent Catalytic System for Converting Carbon Dioxide into Methanol Autocatalytically. *Chem* **2020**, *6* (7), 1742−1754.
(53) Salzinger, S.; Soller, B. S.; Plikhta, A.; Seemann, U. B.; Herdtweck, E.; Rieger, B. Mechanistic studies on initiation and propagation of rare earth metal-mediated group transfer polymerization of vinylphosphonates. *J. Am. Chem. Soc.* **2013**, *135* (35), 13030−13040.
(54) Leute, M. Macromolecules with Phosphorus; Ph. D. Thesis Universitat Ulm: Ulm, 2007.

https://doi.org/10.1021/acsapm.4c02762
ACS Appl. Polym. Mater. 2024, 6, 13855−13864

(55) Giboulot, S.; Comuzzi, C.; Del Zotto, A.; Figliolia, R.; Lippe, G.; Lovison, D.; Strazzolini, P.; Susmel, S.; Zangrando, E.; Zuccaccia, D.; Baldino, S.; Ballico, M.; Baratta, W. Preparation of monocarbonyl ruthenium complexes bearing bidentate nitrogen and phosphine ligands and their catalytic activity in carbonyl compound reduction. *Dalton Trans.* **2019**, *48* (33), 12560−12576.

https://doi.org/10.1021/acsapm.4c02762
ACS Appl. Polym. Mater. 2024, 6, 13855−13864